https://doi.org/10.1245/s10434-026-19351-4 Annals of Surgical Oncology

Integrated Liquid Biopsy and Tumor Tissue Genomic Profiling of Appendiceal Cancer: cfDNA Burden, Mutation Landscapes, and Clinical Outcomes

Sefali Patel[1] · Patricia Petrosko[1] · Phillip H. Gallo[1] · Madeline Myers[2] · Louis Gil[2] · Edward J. Nolan[3] · Seyed H. Hosseiny[3] · Rose Blodgett[1] · Ashten Omstead[1] · Hyun Park[1] · Emily Dalton[4] · Christopher Sherry[1] · Ajay Goel[5] · Casey J. Allen[1] · Ali Zaidi[1] · Russell Schwartz[6,7] · David L. Bartlett[1] · Patrick L. Wagner[1] · William A. LaFramboise[1,2]

Received: 2 October 2025 / Accepted: 10 February 2026

Abstract

Background Appendiceal cancer (AC) is a rare malignancy that often presents at advanced stages with significant histological variability influencing clinical outcomes. Precise genomic profiling is essential for accurate diagnosis and personalized patient management. This study interrogated DNA from appendiceal tumor tissue, buffy coat cells, and the cell-free DNA component of plasma using a 523-gene panel for comprehensive genomic profiling (CGP) to identify cancer-related genetic mutations in tumor and blood, evaluate tumor mutation burden, and determine genetic markers associated with histologic grade.

Patients and Methods A total of 73 patients provided blood samples comprising cell-free DNA (cfDNA) and germline buffy coat cells (bcDNA) for analysis compared with tumor tissues available from 56 of these patients. Concordance of mutations between matched tumor tissue and plasma samples ($n = 51$) was assessed and tumor-specific and germline variants were classified using OncoKB™ clinical criteria to delineate oncogenic and therapeutically actionable variants [level 1 mutations with U.S. Food and Drug Administration (FDA)-approved therapy]. Additionally, cfDNA concentrations were tested for association with clinical and pathologic features and oncologic outcome including disease-specific (DSS) and progression-free (PFS) survival.

Results Circulating tumor DNA (ctDNA) from plasma cell-free DNA demonstrated high concordance with tumor genomic profiling, reaching 98.4% concordance [median, interquartile range (IQR) 13.5, 21.5] overall and 85.7% (IQR 64.6, 100) for therapeutically actionable level 1 mutations. Prevalent appendiceal tumor-specific mutations included KRAS proto-oncogene, GTPase (KRAS) (41%), GNAS complex locus (GNAS) (30%), tumor protein p53 (TP53) (30%), and SMAD family member

✉ Sefali Patel
sefali.patel@ahn.org

1 Allegheny Health Network Cancer Institute, Pittsburgh, PA

2 Allegheny Health Network Pathology Institute, Pittsburgh, PA

3 Highmark Health, Pittsburgh, PA

4 Illumina, Inc., San Diego, CA

5 Department of Molecular Diagnostics and Experimental Therapeutics, City of Hope Comprehensive Cancer Center, Monrovia, CA

6 Ray and Stephanie Lane Computational Biology Department, Carnegie Mellon University, Pittsburgh, PA

7 Department of Biological Sciences, Carnegie Mellon University, Pittsburgh, PA

Published online: 13 March 2026

4 (SMAD4) (29%). Tumor-specific TP53, SMAD4, and spectrin alpha, erythrocytic 1 (SPTA1) mutations strongly correlated with intermediate and high-grade histology, whereas GNAS mutations predominated in low-grade tumors. Germline analysis identified coding mutations shared among this patient cohort in notch receptor 4 (NOTCH4) (55%) and BRCA1 associated RING domain 1 (BARD1) (48%) genes, with zinc finger homeobox 3 (ZFHX3) (29%) and adhesion G protein-coupled receptor A2 (ADGRA2), DNA polymerase epsilon (POLE), and transcription factor 3 (TCF3) mutations (all = 23%) specifically enriched in intermediate and high-grade AC. Both histological grade and cfDNA stratified by concentration tertiles independently predicted progression-free and disease-specific survival. Plasma samples exhibited consistently lower variant allele frequencies than solid tumors, limiting sensitivity for discovery of novel mutations exclusively from plasma.

Conclusions This study supports integrating comprehensive ctDNA assays into standard diagnostic and treatment pathways for AC using large gene panels. TP53, SMAD4, SPTA1, and GNAS mutations serve as prospective tumor-specific molecular classifiers for histological grade, while germline variants in NOTCH4 and BARD1 may further influence disease biology, with ZFHX3, ADGRA2, POLE, and TCF3 affecting grade stratification. Overall cfDNA concentration may serve as a potential prognostic biomarker in AC.

Keywords Appendiceal cancer · Circulating tumor DNA · Cell-free DNA · cfDNA · Comprehensive genomic profiling · Prognostic biomarker · Next-generation sequencing · Ct-TSO500 · Liquid biopsy · Molecular diagnostics · Cancer · Next-generation sequencing · Tumor biomarker

Appendiceal cancer is a rare gastrointestinal malignancy characterized by diverse histopathological features and clinical behaviors that complicate disease assessment and therapeutic management. Accurate, timely detection of progression or recurrence remains challenging due to limitations in traditional surveillance methods such as radiographic imaging and serum tumor markers [e.g., carcinoembryonic antigen (CEA), cancer antigen 19-9 (CA19-9), cancer antigen-125 (CA-125)], especially in patients with low-grade mucinous tumors and those confined to the peritoneum.[1,2] Circulating tumor DNA (ctDNA) analysis via "liquid biopsy" is a promising, minimally invasive method potentially enabling initial tumor diagnosis, detection of minimal residual disease (MRD) during treatment, and surveillance for disease recurrence after therapy while dynamically capturing the genomic landscape of tumors.

Recent evidence supports the clinical utility of ctDNA assays in appendiceal cancer. Belmont et al.[1] reported high sensitivity (93.8%) and specificity (85.0%) for detecting appendiceal cancer recurrence using personalized ctDNA surveillance, often preceding imaging-based identification by several months. However, tissue and "liquid biopsy" concordance remains suboptimal in appendiceal cancer, particularly mucinous and lower-grade subtypes that demonstrate limited ctDNA shedding, thereby hindering detection of the tumor's genomic profile from blood samples alone.[2,3] Consequently, ctDNA assays for these tumors typically require smaller, tumor-agnostic panels (e.g., Guardant360) or personalized tumor-informed assays (e.g., Signatera™) that provide high sensitivity in tradeoff for a limited representation of the tumor's overall genomic complexity.[4]

While histologic grading remains the conventional standard for predicting clinical behavior, emerging evidence underscores the significance of genetic mutational analysis that may independently predict tumor aggressiveness and patient outcomes. Key genomic alterations in KRAS proto-oncogene, GTPase (KRAS), GNAS complex locus (GNAS), tumor protein p53 (TP53), and SMAD family member 4 (SMAD4) demonstrate strong correlations with histological grade and clinical prognosis. Low-grade appendiceal mucinous neoplasms (LAMNs) predominantly exhibit activating KRAS mutations (~74–98%) and frequent GNAS mutations (56–63%), associated with an indolent clinical course.[5] Conversely, high-grade appendiceal adenocarcinomas frequently harbor TP53 mutations (approximately 56%) and SMAD4 mutations (up to 50% in recurrent disease), indicating an aggressive tumor phenotype with a poorer prognostic outcome.[5–7]

Germline pathogenic variants have recently been shown to impact appendiceal adenocarcinoma risk and biology, reinforcing the importance of a comprehensive genomic approach to evaluating patients with appendiceal cancer. Foote et al.[8,9] highlighted approximately 10% of patients with appendiceal adenocarcinoma harboring pathogenic germline variants, primarily in genes involved in DNA damage repair pathways [e.g., BRCA2 DNA repair associated (BRCA2), ATM serine/threonine kinase (ATM), checkpoint kinase 2(CHEK2)]. Germline variants may contribute not only to tumorigenesis, but also in influencing somatic mutation patterns, tumor aggressiveness, therapeutic vulnerabilities, and patient prognosis.[8,9] These findings underscore the need for broad genomic profiling, including germline variant detection, to provide a complete molecular assessment for clinical decision-making and therapeutic planning.

Comprehensive genomic profiling (CGP) of tumors with large NGS panels (> 500 genes) offers significant advantages over small, targeted panels by providing extensive genomic information, including single nucleotide variants (SNVs), insertions/deletions (indels), copy number variations (CNVs), fusions, tumor mutational burden (TMB), and microsatellite

instability (MSI) status. CGP of tumors also facilitates the identification of germline-derived variants, further enriching clinical interpretation and potentially revealing novel therapeutic targets or risk stratification markers that smaller panels may overlook. The purpose of this study was to compare the mutation profiles of DNA from solid tumor (stDNA), peripheral blood cells (buffy coat: bcDNA), and cell-free DNA (cfDNA) of patients with appendiceal cancer who provided samples to our Oncology Sample Biobank and Data Repository for mutation profiling and concordance testing. We standardized blood collection and rapidly processed all samples in the same Allegheny Health Network (AHN) Genomics Facility using our CAP/CLIA approved CGP solid tumor assay and analysis pipeline (TruSight Oncology 500: TSO500 Illumina, San Diego, CA) to uniformly interrogate and compare all specimens while limiting preanalytical and technical variability.[10,11]

Patients and Methods

Consent, Chart Review, and Sample Collection

This study comprised 73 patients (age 24–82 years) diagnosed with appendiceal neoplasms and treated at the Allegheny Health Network (AHN) between 2021 and 2024. The study was approved by the AHN Institutional Review Board (IRB# 2020-258) and performed in accordance with principles of the Declaration of Helsinki. Participants signed a Health Insurance Portability and Accountability Act (HIPAA) authorization and informed consent to provide deidentified information to a database linking their tumor and blood sequencing data with clinicopathological data. The protocol included access to tissues from patients having procedures at one of 21 AHNCI treatment sites and blood samples obtained during routine, clinical lab draws or intravenous therapy at an AHN hospital or clinic.

Whole blood samples were collected in three 10 mL Streck, Cell-Free DNA BCT tubes (Streck, LaVista, NE) according to our standard operating procedure, and the specimens were transported by courier to the AHN Genomics Facility (1307 Federal St. North, Pittsburgh, PA 15212) for processing, DNA purification, sequencing, and analysis.[10] Briefly, blood samples underwent centrifugation in a chilled, swinging bucket rotor at 1600 rcf (Eppendorf 5810R, S-4-104 rotor, 10 min, 4 °C, no brake, Eppendorf, Hamburg, GER). The plasma layer was transferred to a 5 mL conical tube (VWR, Avantor, Radnor, PA) followed by centrifugation in a fixed-angle rotor at 10,000 rcf (Eppendorf 5425R, FA 10 × 5 rotor, 10 min, 4 °C, soft brake). Plasma was transferred to a 5 mL tube and a third spin was performed identically to the previous spin. The plasma and buffy coat were transferred to the AHNCI Biospecimen repository for long-term storage (−80 °C) in 7.6 mL and 1.9 mL FluidX Tricode tubes, respectively (Azenta, Burlington, MA).

Purification of Cell-Free DNA from Plasma for Follow-Up Studies

Cell-free DNA (cfDNA) purification was performed using the Apostle MiniMax High Efficiency cfDNA Isolation Kit (cat. #A17622-250, Beckman Coulter, Indianapolis, IN). The DNA was eluted in 50 µL of elution buffer using magnetic beads and 2 µL were assayed by fluorometry (Qubit Flex, ThermoFisher, Waltham, MA) for concentration using the Qubit dsDNA High Sensitivity kit (cat. #Q32854, ThermoFisher). Quantitative analysis was performed on the 5200 Fragment Analyzer (Agilent, Santa Clara, CA) and software (ProSize Revision 5.0.1.6, Agilent) delineated the DNA fragment size distribution from 75 to 300 bp and 75–1200 bp containing cell-free DNA (cfDNA) typically without "background" germline DNA from lysed cells identifiable in larger fragments if present. Percentages of each region were multiplied by Qubit Flex quantitation values to obtain the concentration of these DNA components per sample.

Purification of DNA from FFPE Specimens

Formalin-fixed, paraffin embedded, tumor tissues were acquired from pathology blocks as cores (1 mm by 0.5 cm punch biopsy) or 10–20 slides of unstained sections (5–10 µm thickness). Tumor regions were demarcated by a pathologist and removed from deparaffinized unstained slides using a scalpel (Penblade-size 10, 15, 22, ThermoFisher) in register with a hematoxylin and eosin (H&E) stained slide. Tumor tissue was collected (2 mL, Eppendorf, Hauppauge, NY) and dehydrated in 500 µl xylene, after which xylene was removed by centrifugation (Eppendorf Minispin plus, 1000 rcf × 2 min) and the samples mixed in 100% ethanol (Pharmco, Brookfield, CN). The centrifugation process was repeated; the ethanol supernatant was removed from the pellet and the samples were allowed to dry. DNA was extracted (FormaPure XL TNA FFPE Extraction kit, Beckman Life Sciences, Indianapolis, IN) according to the Beckman FormaPure XL Manual Extraction Protocol (doc. #158133.2, Beckman) and the stDNA assessed for purity (NanoDrop, ThermoFisher), quantified by fluorometry (Qubit Flex, ThermoFisher) and fragment size, and integrity measured by capillary electrophoresis (5200 Fragment Analyzer, Agilent). Samples were subjected to fragmentation if they contained ≥ 40 ng with fragment sizes > 90 bp in the 80–20,000 bp range.

Purification of DNA from Buffy Coat Samples

Buffy coat DNA was purified with the column-based QuickDNA™ Midiprep Plus Kit (D4075, Zymo Research, Irvine, CA) according to the manufacturer's protocol. Purified DNA

was evaluated for purity and quantity as previously described for cell-free and solid tumor DNA. An aliquot of bcDNA was diluted to 3 ng/ul for analysis by capillary electrophoresis (5200 Fragment Analyzer, HS Genomic DNA Kit: DNF-488, Agilent) and underwent fragmentation due to a genomic size distribution routinely exceeding 20 kb.

Library Preparation of Solid Tumor, Buffy Coat, and Cell-Free DNA Samples

Sequencing libraries were prepared from stDNA and bcDNA according to the Illumina TruSight Oncology 500 Reference Guide (doc. #1000000067621 v10, July 2022, Illumina, San Diego, CA). DNA underwent end repair, A-tailing, and adapter binding reactions including addition of unique molecular identifiers (UMIs) through an "index" polymerase chain reaction (PCR) amplification step (15 cycles: 10 s at 98 °C, 30 s at 60 °C, 30 s at 72 °C) to obtain 80 ng/µl. Genomic targets were selected by serial hybridization–capture enrichment reactions using streptavidin magnetic beads (12 h at 57 °C). DNA libraries were pooled ($n = 8$) and manually normalized to 1.1 pM according to the NextSeq System Denature and Dilute Libraries Guide (doc. #15048776 v16, July 2020, Illumina) followed by paired-end sequencing (2 × 100 bp or 2 × 150 bp) on the NextSeq 550Dx according to the NextSeq550 Sequencing Systems protocol (doc. #15069765 v07, Oct. 2021, Illumina), including DNA reference samples as assay controls.

Libraries from cfDNA underwent sequencing following the Illumina TruSight Oncology 500 ctDNA Reference Guide (doc. 1000000092559 v00 February 2020, Illumina). Briefly, a minimum of 25–30 ng cfDNA contained within the 75–300 bp DNA domain was required. Library preparation included end repair, A-tailing, UMI addition, adapter ligation, and index PCR yielding a concentration of approximately 80 ng/µl. Serial target enrichment was performed followed by PCR to obtain fragments in the 325–350 bp range at a concentration of 20 ng/µL. A total of 24 libraries were manually normalized (0.65 nM) and paired-end sequencing (2 × 150 bp) was performed on the NovaSeq 6000 according to the Sequencing System Guide (doc. #1000000019358 v17 Sept. 2022, Illumina).

Data Analysis Pipeline

Tumor and buffy coat binary base call (BCL) files were generated by the NextSeq Local Run Manager (LRM: TruSight Oncology 500 v2.2 software; Doc. #10000000151997 v01, September 2021, Illumina) including read collapsing and error correction. BCL files were aligned to form FASTQ files (BWA: Burrows-Wheeler Aligner: HG19 reference) followed by local realignment for insertions or deletions (indels) and paired end stitching using the GEMINI software module. Single nucleotide variants (SNV) and indels were called by PISCES software, multiple nucleotide variants (MNV) by SCYLLA, and copy number variants (CNV) by the CRAFT program. Small variants were filtered at read depth ≥ 100 reference calls and 1% variant allele frequency (VAF) as the analytical limit of detection. Variant call files (VCF) were annotated by the Nirvana Annotation Engine against public databases (dbSNP, gnomAD, 1000 genomes, ClinVar, RefSeq, Ensembl). Tumor mutation burden (TMB) was generated from small variant files across 1.33 Mb of exonic sequence after removing germline variants using TMBRaider software. Mutation annotation format (MAF) files were created from JavaScript Object Notation (JSON) files to interrogate the OncoKB™ Oncology Knowledge Database (v4.9) for pathogenicity and clinical actionability of variants for U.S. Food and Drug Administration (FDA)-approved level 1 oncology drugs dating back to 1998.[12] Cell-free DNA libraries sequenced on the NovaSeq6000 (Illumina) were processed in Illumina Connected Analytics (ICA) using the DRAGEN TruSight Oncology 500 ctDNA Analysis software v1.2 (Doc. #200015532 v00, August 2022). Analysis followed the LRM processing paradigm incorporating the DRAGEN aligner followed by stretched realignment using GEMINI. SNVs and indels were called by PISCES, MNVs by SCYLLA, and CNVs by the CRAFT module. Clonal hematopoietic variants of indeterminate potential (CHIP) in cfDNA (< 1% VAF) were removed using matched germline and/or Genome Aggregation Database (gnomAD) of population frequencies (< 0.001). TMB was defined using TMBRaider software. NIRVANA generated annotations using the same databases as solid tumors. Small variants underwent post-processing filtering for read depth cutoff at 500 reference calls and 0.1% variant allele frequency (VAF) as the analytical limit of detection. MAF files were created from cfDNA JSON files to interrogate the OncoKB™ Oncology Knowledge Database (v4.9) as described previously.

Statistical Analysis

Correlation analysis between solid tissue and circulating tumor data was employed to define shared and exclusionary variants. Variants within combined domains of the Dragen stDNA and cfDNA "blacklists" indicating genomic regions prone to high background noise were removed, and missense, frameshift, stop-gained, splice region, splice donor, and inframe deletions were processed in R using a merging function on the basis of chromosome start and end position, reference allele, altered allele, and lower limit of detection to identify mutations in common. There was no Dragen blacklist for bcDNA sequencing, thus each germline variant was visually inspected using the Integrative Genomics Viewer (IGV) to detect errant SNV calls due to mismatched

alignment, strand bias, or ambiguously identified reads.[13] A subsequent "anti-join" function was used to identify mutations unique to the solid tissue, buffy coat, or circulating tumor DNA. Concordance was calculated by dividing the total number of variants shared between each plasma and tumor tissue pair by the total number of variants detected in the matched solid tumor.

Normality of data distribution was evaluated using the Kolmogorov–Smirnov and Shapiro–Wilk tests. Between-group differences for normally distributed data were analyzed by *t*-test and analysis of variance (ANOVA) while nonnormally distributed data were analyzed by the Mann–Whitney *U* test and Kruskal–Wallis test. Association between continuous variables was assessed using Spearman's rank correlation test. Additionally, test characteristics including sensitivity, specificity, and positive and negative predictive values were computed for cell-free DNA to predict concordance with therapeutically actionable mutations present in solid tumors. Survival outcomes were compared among subgroups using Cox proportional hazard regression. Statistical analysis was performed using SAS (version 9.4) or STATA (StataCorp, College Station TX, version 17.0) and statistical significance was defined at an alpha error level $(p) < 0.05$.

Results

Patient Population and Clinical Characteristics

A range of appendiceal tumor histotypes were represented among the 73 patients in this study, with an even distribution across histological tumor grades (low or grade I: $n = 23$, intermediate or grade II: $n = 22$, high or grade III: $n = 28$) (Table 1). Most patients (86%) had disseminated disease with peritoneal carcinomatosis, and among these patients the median peritoneal carcinomatosis index (PCI) was 21 (IQR 14, 31) (Table 1). Blood samples were collected while controlling for critical preanalytical variables of time, temperature, and agitation during transfer such that 92% of these specimens (67 of 73) were converted to plasma and in storage at −80°C within 27 h of the blood draw time (mean ± STDEV = 19.0 ± 18.6 h).[10] The cfDNA concentrations obtained from these samples revealed a probability distribution that rejected the hypothesis of normality due to extremes in concentration values (Kolmogorov–Smirnov: KS distance = 0.238; $p \leq 0.001$, Shapiro–Wilk: W = 0.692; $p \leq 0.001$). The overall median cfDNA concentration was 6.43 ng/mL (IQR 3.70, 9.55 ng/mL), spanning a wide range from 1.16 ng/mL to 49.9 ng/mL (Fig. 1). The cfDNA concentrations did not show a statistically significant correlation with age, histotype, PCI, American Joint Committee on Cancer (AJCC) stage, histological grade, or nodal status during multivariable correlation analysis.

Survival Analysis and cfDNA Concentration

As expected, histological grade strongly correlated with the clinical outcomes of progression-free survival (PFS) and disease-specific survival (DSS) in our patients, consistent with previous studies (Fig. 2A,B).[14] Increasing cfDNA concentrations also predicted adverse clinical outcomes, including shorter progression-free survival (PFS) and reduced disease-specific survival (DSS) when compared across cfDNA concentration tertiles (0.9–4.1 ng/mL,4.3–7.8 ng/mL; 8.4–49.9 ng/mL; Fig. 2C,D). Patient samples in the lowest concentration range had a significantly different PFS from patients in the intermediate ($p \leq 0.05$, hazard ratio, HR 0.355, 95% CI 0.14, 0.89) and high ($p \leq 0.01$, HR 0.295, 95% CI 0.12, 0.72) concentration range (Fig. 2C). There was no significant difference in PFS between patients in the intermediate and high concentration groups based on cfDNA concentrations. An identical pattern of statistical significance with increased cfDNA concentration was also present for cfDNA and DSS with no significant difference between the intermediate and high concentrations (low versus intermediate: $p \leq 0.05$, HR 0.377, 95% CI 0.15, 0.93; low versus high: $p \leq 0.02$, HR 0.319, 95% CI 0.13, 0.77; Fig. 2D). It is important to note that the association of cfDNA concentration with the occurrence of adverse events in PFS and DSS was independent of histological grade. Specifically, there was no significant statistical correlation detected between the variables of cfDNA and histological grade when compared using the Kruskal–Wallis test (K value = 3.79, critical value = 5.99, $p = 0.1502$) and this extended to multiple variables in the study when tested by multivariable Cox proportional hazards regression analysis including age, sex, histotype, AJCC stage, and histological grade. We also tested for a relationship of PCI values to cfDNA, variant counts, and tumor mutation burden for the 43 cases where we had overlapping values. The results indicated that no statistically significant correlations existed between PCI and these variables (cfDNA: $p = 0.2056$, total variants: $p = 0.9653$, coding variants: $p = 0.8864$, OncoKB™ variants: $p = 0.9885$, tumor mutation burden: $p = 0.1717$).

Genomic Variant Profiling and Concordance Analysis

We obtained residual, primary tumor specimens for 56 of 73 patients for identification and comparison of stDNA mutations with patient germline (bcDNA) variants. Each patient was individually curated for the time of procurement of their diagnostic blood and matched tumor specimen to discriminate any therapeutic interventions (surgery, chemo-, immuno-, radiotherapy) that took place between acquisition

Table 1 Patient clinical characteristics

Patient Characteristics		Number (%)
Age (years): Median (IQR)	53 (46–61)	73
Sex ($n = 73$)	Male	46 (63%)
	Female	27 (37%)
Histologic grade ($n = 73$)	LOW (I)	23 (32%)
	INTERMEDIATE (II)	22 (30%)
	HIGH (III)	28 (38%)
Histotype ($n = 72$)	Low-grade mucinous neoplasm	14 (19%)
	Mucinous adenocarcinoma	30 (42%)
	Goblet cell carcinoma	11 (15%)
	Signet ring cell carcinoma	8 (11%)
	Adenocarcinoma (not specified)	9 (13%)
AJCC stage (72)	1	1 (1%)
	2	7 (10%)
	3	2 (3%)
	4	62 (86%)
CEA (ng/mL): Median (IQR) ($n = 64$)	4.4 (1.8–15.4)	64
Nodal Involvement ($n = 52$)	None	30 (58%)
	Present	22 (42%)
Peritoneal Carcinomatosis Index (PCI): Median (IQR) ($n = 58$)	21 (14–31)	58
Lymphovascular Invasion ($n = 23$)	None	17 (74%)
	Present	6 (26%)
Perineural Invasion ($n = 20$)	None	7 (35%)
	Present	13 (65%)

Key patient characteristics including age, sex, histological grade, tumor histological type (histotype), AJCC stage, nodal status, and biomarkers such as carcinoembryonic antigen (CEA) and peritoneal carcinomatosis index (PCI) are annotated. Data are presented as median and interquartile 1 and 3 values. Most patients were male (63%) and the entire patient cohort had a median age of 53 years. The predominant histology was mucinous adenocarcinoma (42%), and most cases were stage AJCC 4 (86%). Relevant pathological findings include nodal involvement (42%), lymphovascular invasion (26%), and perineural invasion (65%). Data availability for each variable is noted by the number of patients evaluated for each parameter (*n* patient number).

IQR interquartile range. *AJCC* American Joint Committee on Cancer, *CEA* carcinoembryonic antigen

of the samples (Table 2). There were 51 cases with tumor and blood specimens acquired sufficiently close in time and absent an intervening change in therapy, with plasma samples suitable for concordance testing of cfDNA versus stDNA variants. Figure 3A delineates the time elapsed from each blood draw to plasma conversion for the 51 concordance samples, indicating that 92% were processed within 27 h of blood collection and 44 cases (86%) comprised blood samples drawn the morning of the tumor biopsy or resection procedure (Fig. 3B). Every plasma sample in this study produced a sufficient yield of cfDNA (≥ 25 ng) and was sequenced successfully on the CGP panel.

The SNVs and indels generated during concordance testing did not conform to a normal distribution and were subjected to nonparametric analysis (all common variants: Kolmogorov–Smirnov: KS distance = 0.792; $p \leq 0.001$, Shapiro–Wilk: W = 0.204; $p \leq 0.001$). Detection of solid tumor variants within ctDNA was notable, capturing a median value of 98.4% of overall variants identified in stDNA (Table 2). Both assays concurrently detected more than a thousand variants overall per patient (MED 1116.0; IQR 1074.0, 1149.5), including 159.0 nonsynonymous, coding mutations (IQR 155.0, 168.5). Every patient in the cohort harbored at least one oncogenic mutation identified in the OncoKB™ clinical database, with a median of 7.0 (IQR 5.0, 8.0) oncogenic variants per case and a median concordance of 85.7%. Clinically "actionable" genomic alterations were identified in both tumors and blood of 25 of the 51 patients (49.0%) as targets for established pharmacotherapies (Table 2), while 19 patients had oncogenic mutations detected by both assays without an associated pharmacological therapy (Table 2). Three patients had actionable mutations identified in the stDNA only, while four patients had actionable mutations detected only by the ctDNA assay. Spearman's correlation analysis revealed a significant relationship for oncogenic mutations detected in

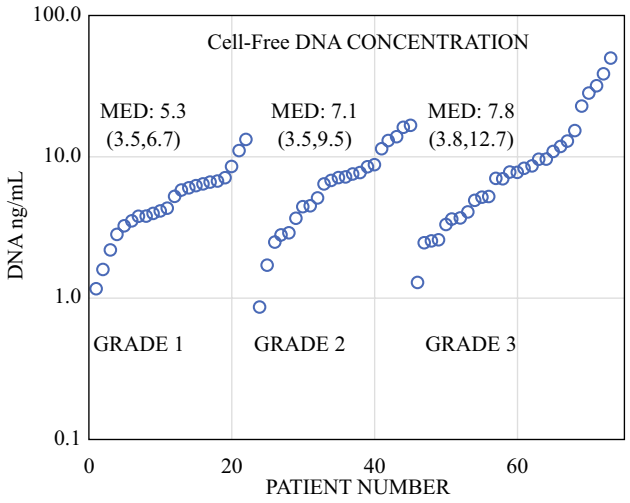

Fig. 1 Cell-free DNA concentrations in patients with appendiceal cancer; cell-free DNA was quantified for the 73 patients in this study on the basis of the 75–1200 base pair range (see Methods) and the results are plotted logarithmically on the vertical axis; individual patient concentrations are reported from smallest to largest value for cohorts on the basis of tumor grade; *MED* median (interquartile 1, interquartile 3)

stDNA and ctDNA datasets within the OncoKB™ clinical database (OncoKB: $r = 0.69$, $p < 0.001$) with a concordance of 94.1% in determining therapeutic actionability across all 51 patients. These results provided clinical sensitivity for the ctDNA assay of 90.6% to detect actionable mutations with specificity, accuracy, and positive predictive value of 100%.

Tumor-Specific and Germline Mutations in Appendiceal Cancer

Germline variants were identified and subtracted from tumor profiles and nonsynonymous, coding variants were crossed with the OncoKB™ database to identify mutations relevant to cancer in 56 patients (Fig. 4). Multiple tumor-specific mutations within an individual gene and patient were collapsed to indicate whether patients were positive for oncogenic mutations within each gene. These data were then accumulated across the entire patient cohort. The most frequent tumor-specific gene mutations across the patient cohort were in KRAS (41.1%), GNAS (30.4%), TP53 (30.4%), SMAD4 (28.6%), spectrin alpha, erythrocyte 1 (SPTA1) (14.3%), and ATM (10.7%) genes (Fig. 4A). The number of unique tumor mutations per gene across the cohort ranged from 3 variants in GNAS shared among 17 patients to 15 distinct mutations in TP53 that were distributed among 23 members of the cohort.

Germline mutations were similarly compared against the OncoKB™ database for cancer relevance. Nonsynonymous germline mutations in notch receptor 4 (NOTCH4) (55.4%) and BRCA1 associated RING domain 1 (BARD1) (48.2%) (Fig. 4B) were identified at levels exceeding the highest tumor specific mutations. It is noteworthy that 27 patients shared a BARD1 missense mutation (23 heterozygous, 4 homozygous) comprising MNV (chr 2; g. 215632255-215632256delCAinsTG; NM_000465.3: p.Val507Met) identified in ClinVar (rs386654966) as potentially pathogenic and associated with a familial predisposition to breast cancer. Similarly, 25 of the 31 patients with a NOTCH4 mutation shared MNV (rs71556915: chr 6: g.32188640-32188642delTCTinsCCC; NM_004557.4: p.Asp272Gly) identified in the Catalogue of Somatic Mutations in Cancer (COSMIC) (COSV105931127) associated with stomach tumors. Approximately a quarter of these patients exhibited germline mutations in zinc finger homeobox 3 (ZFHX3) (28.6%), transcription factor 3 (TCF3), DNA polymerase epsilon, catalytic subunit (POLE), and BRCA2 genes (all at 23.2%) (Fig. 4B). It is important to note that these germline mutations were also detected in the cfDNA, requiring that sequencing of buffy coat blood cells be performed for unequivocal tumor versus germline variant identification and to discriminate CHIP variants from tumor-specific mutations at low VAF levels. Overall, these results validated the robust utility of comprehensive genomic profiling from tumors and "liquid biopsy" assays for detection of clinically relevant diagnostic and therapeutic alterations and underscored the diagnostic significance of ctDNA monitoring in appendiceal cancer.

Mutation Profiles of Histologic Low-Grade versus High-Grade Tumors

We interrogated somatic mutation profiles across tumor grade, consolidating grade 2 tumors with grade 3 tumors as high-grade for comparison with grade 1 or low-grade tumors. In keeping with prior studies,[5–7] GNAS mutations were strongly associated with low-grade histology, whereas TP53 was associated with high-grade histology when a chi-squared test of independence was applied across mutations and grade (both $p \leq 0.001$) (Fig. 5A). Germline variants were evenly distributed across this patient cohort, including NOTCH4 and BARD1, except for ZFHX3 mutations, which were in a third (35.1%) of the high-grade patients but only three of the low-grade tumors (chi-squared test: $p \leq 0.05$). Similarly, variants in adhesion G protein-coupled receptor A2 (ADGRA2), POLE, and TCF3 were in more than a quarter (27.0%) of the patients with high-grade tumors but did not reach statistically significant discrimination from low-grade patient frequencies (Fig. 5B). Neurotrophic receptor tyrosine kinase 1 (NTRK1) and SLX4 structure-specific endonuclease subunit (SLX4) gene mutations were the only variants that demonstrated the opposite trend of a statistically significant elevation in low-grade tumors (NTRK1:

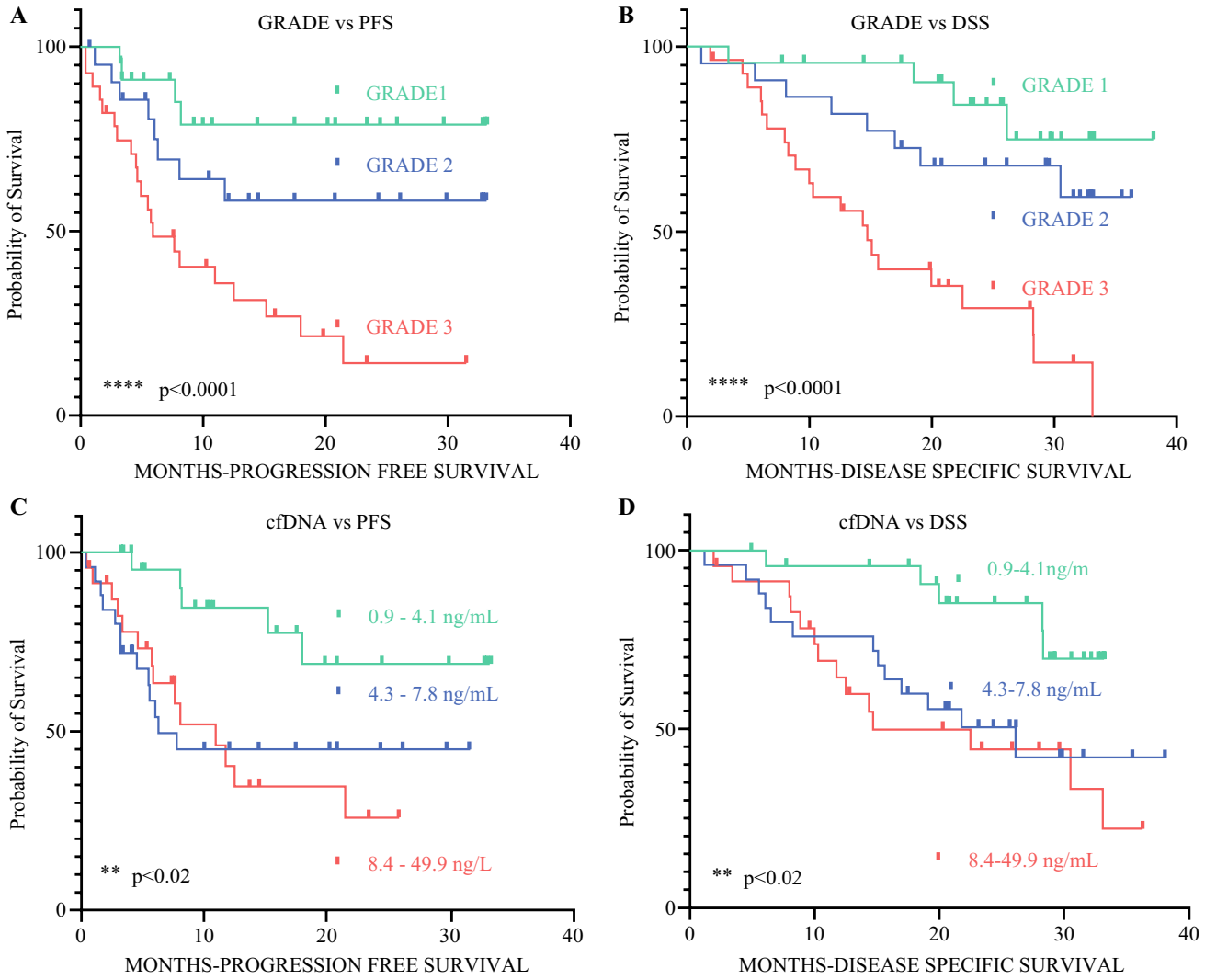

Fig. 2 Kaplan–Meier survival probability curve versus histological grade or cfDNA concentration; **A** progression-free survival curves plotted for three cohorts on the basis of tumor histological grade, statistical significance was derived from log-rank survival analysis, grade is listed adjacent to each individual curve (GRADE) (see Supplementary Table 1 for hazard ratios generated for the KM plots in Figs. 2A,B,C,D); **B** disease-specific survival curves plotted for the same cohorts as in (**A**) on the basis of tumor histological grade, PFS and DSS progressively declined across cohorts on the basis of increasing grade (chi-squared: $p < 0.0001$); **C** cfDNA tertile concentrations of initial blood samples were subjected to survival analysis on the basis of progression-free survival as in Fig. 2A, the range of individual patient cfDNA concentrations within each cohort are provided next to their respective curves; **D** cfDNA tertile concentrations underwent survival analysis on the basis of disease-specific survival times as in Fig. 2C; both PFS and DSS prognosis progressively declined across cohorts on the basis of increasing cfDNA concentration values (chi-squared: $p < 0.05$)

low-grade = 31.6%, high-grade = 10.8%; $p \leq 0.05$; SLX4: low-grade = 26.3%, high-grade = 8.1%; $p \leq 0.05$) (Fig. 5B). The top ranked classifier for tumor-specific mutations that discriminated low-grade versus high-grade tumors using the Bernoulli Naïve Bayes algorithm for binary data (mutation presence versus absence) comprised mutations in GNAS, NOTCH1, SMAD4, and tet methylcytosine dioxygenase 1 (TET1), which had an area under curve (AUC) of 0.924 (Fig. 6). No germline classifier exceeded an AUC of 0.697 in the ability to distinguish low- versus high-grade tumors nor did the addition of germline mutations to the tumor-specific classifier increase the AUC value obtained from tumor mutations alone.

Discussion

This study evaluated the clinical efficacy of comprehensive genomic profiling of circulating tumor DNA (ctDNA) from patients with metastatic appendiceal cancer (AC). The results demonstrated robust performance of the TSO500 assay for ctDNA variant detection, supporting its

Table 2 Concordance of variants from matched tumors and plasma detected by comprehensive genomic profiling

	ALL VAR				CODING VAR				Onco KB VAR			
VALUE	BOTH	CF ONLY	ST ONLY	CONCRD	BOTH	CF ONLY	ST ONLY	CONCRD	BOTH	CF ONLY	ST ONLY	CONCRD
MED	1116.0	24.0	17.0	98.4%	159.0	9.0	5.0	97.5%	7.0	3.0	1.0	85.7%
IQR1	1074.0	18.5	13.5	98.1%	155.0	6.5	2.0	94.9%	5.0	1.0	0.0	64.6%
IQR3	1149.5	33.5	21.5	98.8%	168.5	14.5	8.0	98.8%	8.0	4.0	3.0	100.0%
AVE	1127.2	28.0	28.0	97.7%	163.7	10.4	6.9	96.2%	6.7	2.9	1.7	82.3%
STDEV	80.5	15.1	57.0	3.7%	14.7	5.7	12.1	5.0%	2.0	2.4	1.9	18.9%
									LEVEL 1 THERAPEUTIC n=51			
									BOTH	CF ONLY	ST ONLY	NONE
									25	4	3	19

implementation as an integral part of personalized therapeutic strategies in appendiceal cancer management. The concordance rate between matched solid tumor DNA and ctDNA exceeded previously published rates for appendiceal tumors (approximately 79–88%) derived from smaller targeted gene panels and tumor-informed assays.[1–3] Notably, our findings demonstrated exceptional concordance for coding mutations (96.2%), high sensitivity to detect clinically actionable mutations (90.6% sensitivity) among our patients, and excellent utilization evidenced by successful sequencing of every plasma sample acquired for concordance testing. High concordance and sensitivity are particularly crucial in appendiceal cancer, a disease expected to shed comparatively low quantities of DNA into the circulation, making ctDNA detection historically challenging.[1,4]

These results reinforced the strong diagnostic and prognostic value of ctDNA in appendiceal cancer, especially regarding outcomes of recurrence and survival. Elevated cfDNA concentrations independently predicted significantly shorter progression-free and disease-specific survival across the wide spectrum of cfDNA concentrations detected in this study. These findings align with recent multicenter studies and clinical trials, including data from Belmont et al.[1], who demonstrated that ctDNA positivity post-cytoreductive surgery significantly correlated with shorter recurrence-free survival intervals (median 11.3 months versus not reached; HR ~14, $p = 0.01$). Similarly, Dhiman et al.[2] found rising postoperative ctDNA to be an early and powerful indicator of recurrence, predicting relapse with approximately 90% accuracy, significantly earlier than conventional imaging or tumor markers such as CEA or CA19-9. The current study reinforces the prognostic power of ctDNA detection from samples collected under a standardized protocol to reduce preanalytical sample variability, and supports its integration into post-treatment monitoring, allowing for timely clinical interventions before overt recurrence.

Prior studies have highlighted the complexity of correlating PCI scores with ctDNA due to the unique tumor biology of appendiceal cancer, particularly mucinous subtypes that often exhibit large tumor burdens without proportionate ctDNA release. Large-scale genomic studies by White et al.[4] and Foote et al.[8,9] similarly noted a disconnect between PCI scores and ctDNA detection rates. White et al. emphasized that tumor histologic aggressiveness, rather than absolute tumor volume, strongly correlates with plasma ctDNA positivity—only 38% of appendiceal adenocarcinomas yielded detectable ctDNA despite extensive peritoneal disease in their study. Consequently, PCI alone may not reliably predict ctDNA detection, suggesting that clinicians should interpret ctDNA in the broader context of tumor biology and disease behavior rather than tumor volume alone.

Actionable mutations, including KRAS, GNAS, and TP53, were consistently detected in the tumors of our patients corroborating prior studies.[4,8,9,15–17] We also identified germline, nonsynonymous, coding mutations throughout the patient cohort in BARD1 and NOTCH4 genes previously implicated in a variety of cancers including breast and stomach cancer, respectively.[18,19] These singular, shared mutations were almost exclusively heterozygous in nature but suggest a predisposition to increased cancer risk, particularly regarding the tumor suppressor role contributed by these genes. Elevated cfDNA levels correlated with aggressive tumor phenotype including frequent TP53 and SMAD4 mutations consistent with established roles in tumor biology. In contrast, tumor-specific GNAS mutations were found predominantly in low-grade tumors. These findings reinforced established correlations of genetic mutations with tumor grade and clinical prognosis. Specifically, mutations in TP53 and SMAD4 were robust markers of aggressive disease and poor prognosis, whereas GNAS mutations reliably indicated low-grade tumors with a favorable clinical trajectory.[5–7,20]

Germline mutations in ZFHX3 were present in a third of the patients with intermediate and high-grade tumors, suggesting the presence of an inherited predisposition that may influence appendiceal cancer aggressiveness and treatment responsiveness, supporting the integration of germline

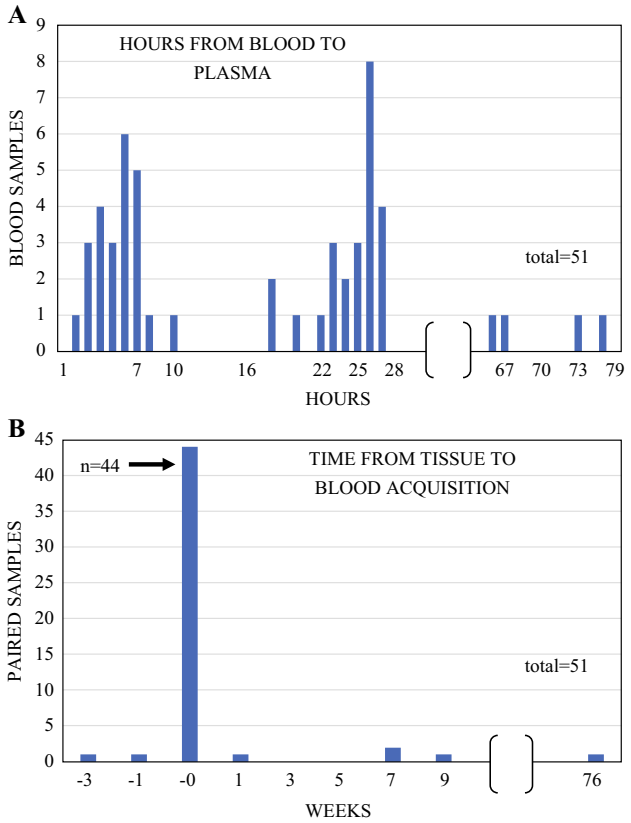

Fig. 3 Blood to plasma processing intervals and time proximity of matched blood and tissue acquisition; **A** processing of whole blood specimens: vertical bars indicate the time differential required to process each of the 51 blood samples for concordance analysis from the time of draw to plasma from the inception of this study, 1 June 2021; the zero timepoint represents the time of the blood draw; 92% of blood samples (92.2%) were processed to plasma within 27 h of the patient's blood draw; brackets on the abscissa indicate a compressed time when no plasma samples were processed for this study; **B** differences in matched specimen procurement: vertical bars indicate the number of blood samples collected at each timepoint compared with acquisition of the surgical specimen in the tumor-blood concordance studies; a negative or a zero value on the abscissa (46 of 51 patients) indicates blood samples obtained prior to acquisition of tumor tissue, while the 5 positive numerical samples were collected after the tissue was acquired; the highest bar reflects the 44 blood samples that were acquired on the same day immediately prior to the biopsy or surgical procedure antecedent to anesthesia and surgery protocols; brackets on the abscissa indicate a compressed time when no plasma samples were processed for this study

profiling in future risk stratification and treatment planning.[8,9] Mutations in GNAS, NOTCH1, SMAD4, and TET1 were important contributors to a low- versus high-grade classifier signature derived from our data. We recognize that the numbers underlying this classifier were limited, and subsequently tested this signature using data from the cBioPortal comprising low- and high-grade appendiceal tumors ($n = 113$), resulting in AUC = 0.77.[21] These findings suggest that further refinement of a predictive signature may be achieved even in this rare cancer, if sufficient precisely annotated clinical specimens with validated CGP results can be accumulated.

Despite the high concordance of actionable mutations between solid tumor and cell-free DNA, plasma-based ctDNA assays demonstrated lower sensitivity for detecting novel variants due to reduced lower ctDNA variant allele frequencies (VAFs). Additionally, mutations outside of the germline were consistently found exclusively in either plasma or tumor tissue samples. These may arise due to formalin fixation affecting tumor DNA integrity and overall tumor heterogeneity, or derive from evolving metastases or other undetected primary tumors in patients, suggesting the necessity for multimodal genomic assessments. Ongoing research indicates that combining plasma and peritoneal fluid sampling after cytoreductive surgery or intraperitoneal chemotherapy may improve detection accuracy, particularly in cases of peritoneal-only disease, where plasma shedding may be limited.[3,22] Future research should explore integrating ctDNA and peritoneal lavage fluid analyses to improve sensitivity and guide postoperative surveillance more effectively. Prospective studies and clinical trials currently underway are evaluating the clinical impact of ctDNA-directed adjuvant therapies in appendiceal cancer, potentially shifting clinical practice toward molecular-driven, personalized management strategies.

The findings of this study support ctDNA as a valuable clinical biomarker in appendiceal cancer management. Specifically, comprehensive ctDNA assays such as the TSO500 could enable (a) real-time molecular profiling for identification of actionable therapeutic targets, (b) risk stratification based on mutational burden and ctDNA persistence, and (c) early identification of minimal residual disease post-surgery, allowing for timely intervention. In conclusion, our results emphasize the clinical utility of comprehensive ctDNA assays for prognosis, treatment selection, and surveillance in appendiceal cancer. Further integration of ctDNA analysis into clinical practice could significantly enhance personalized treatment strategies, ultimately improving patient outcomes.

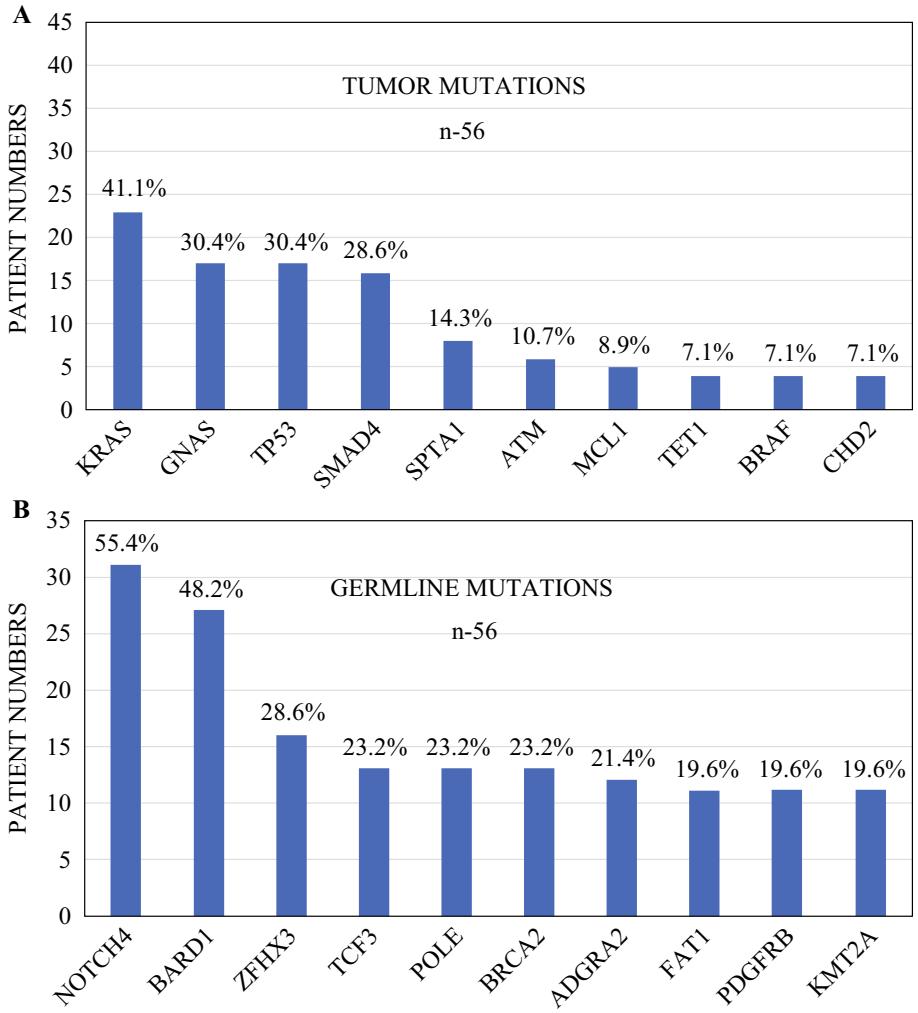

Fig. 4 Appendiceal tumor and genomic variants; **A** tumor-specific mutations detected in appendiceal tumors: the vertical bars indicate the number of patients of the 56 evaluated with tumors containing at least one oncogenic mutation on the basis of the OncoKB database, for the gene specified on the horizontal axis; at the top of each bar is the percentage value for patients in the cohort that contained the mutation; these mutations were obtained after removal of the germline variants delineated in panel B; gene abbreviations and approved names according to HGNC nomenclature include KRAS proto-oncogene, GTPase (KRAS), GNAS complex locus (GNAS), tumor protein 53 (TP53), SMAD family member 4 (SMAD4), spectrin alpha, erythrocytic 1 (SPTA1), ATM serine/threonine kinase (ATM), MCL1 apoptosis regulator (MCL1), BCL2 family member, tet methylcytosine dioxygenase 1 (TET1), B-Raf proto-oncogene (BRAF), serine/threonine kinase, and chromodomain helicase DNA binding protein 2 (CHD2); **B** germline mutations detected in appendiceal tumors: the vertical bars indicate the number of patients with germline mutations detected in their buffy coat blood cells containing at least one oncogenic mutation on the basis of the OncoKB database, for the gene specified on the horizontal axis; at the top of each bar is the percentage value for patients in the cohort that contained the mutation; gene abbreviations and approved names according to HGNC nomenclature include notch receptor 4 (NOTCH4), BRCA1 associated RING domain 1 (BARD1), zinc finger homeobox 3 (ZFHX3), transcription factor 3 (TCF3), DNA polymerase epsilon (POLE), catalytic subunit, BRCA2 DNA repair associated (BRCA2), adhesion G protein-coupled receptor A2 (ADGRA2), FAT atypical cadherin 1 (FAT1), platelet-derived growth factor receptor beta (PDGFRB), and lysine methyltransferase 2A (KMT2A)

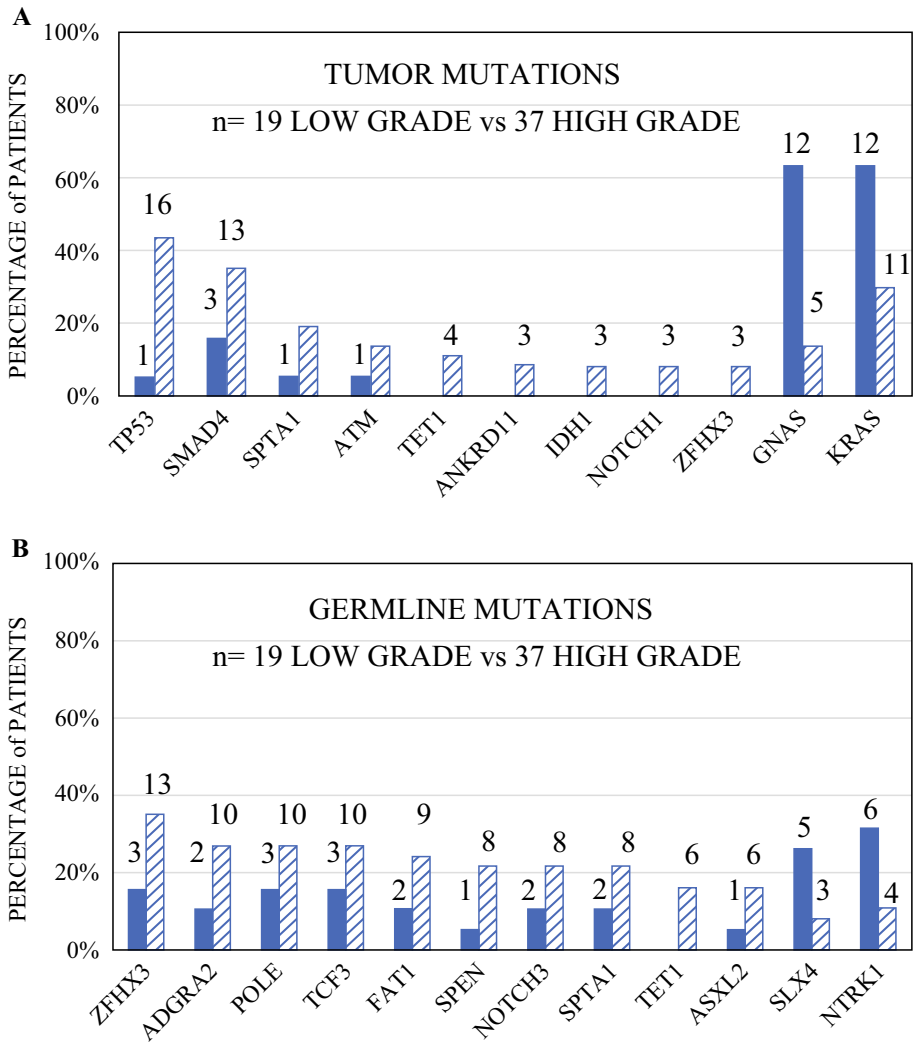

Fig. 5 Low- versus high-grade tumor genomic variants; **A** tumor-specific mutations detected in low- versus high-grade appendiceal tumors; the solid vertical bars indicate the percentage of patients with low-grade tumors ($n = 19$ total) containing at least one tumor-specific oncogenic mutation on the basis of the OncoKB database, for the gene specified on the horizontal axis; above each bar is the actual number of patients within that cohort that had each mutation; the bars with diagonal lines are percentages associated with high-grade tumors ($n = 37$ total); these mutations were obtained after removal of the germline variants delineated in panel B; gene abbreviations and approved names according to HGNC nomenclature are specified in Fig. 2 with the addition of ankyrin repeat domain containing 11 (ANKRD11), isocitrate dehydrogenase (NADP (+)) 1 (IDH1), and notch receptor 1 (NOTCH1); **B** germline mutations detected in low- versus high-grade appendiceal tumors; the solid vertical bars indicate the percentage of patients with low-grade tumors containing at least one germline oncogenic mutation on the basis of the OncoKB database as shown in Fig. A; the numbers above each bar are actual patient numbers and the bars with diagonal lines are associated with high-grade tumors; gene abbreviations and approved names according to HGNC nomenclature are specified in Figs. 2 and 3A with the addition of FAT atypical cadherin 1 (FAT1), spen family transcriptional repressor (SPEN), notch receptor 3 (NOTCH3), ASXL transcriptional regulator 2 (ASXL2), SLX4 structure-specific endonuclease subunit (SLX4), and neurotrophic receptor tyrosine kinase 1 (NTRK1)

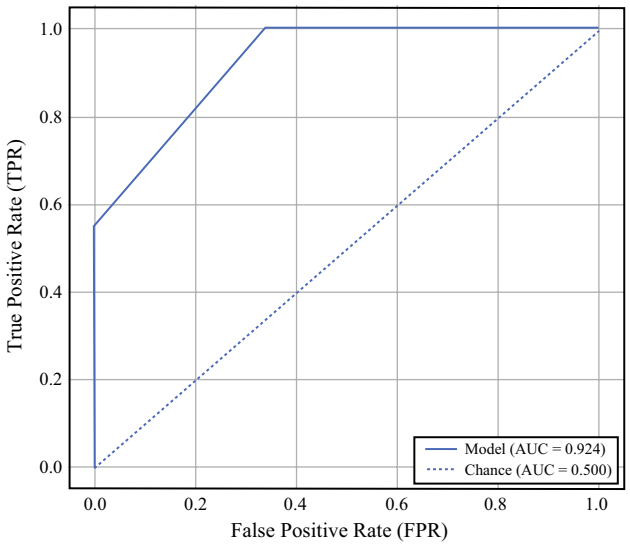

Fig. 6 Classifier model performance; receiver operating characteristic curve of Bernoulli Naïve Bayes classifier for tumor-specific mutations between low- and high-grade tumors; receiver operating characteristic (ROC) curve of a Bernoulli Naïve Bayes classifier trained using complete subsets modeling upon a 70% stratified training set ($n = 39$) and tested upon a 30% test set ($n = 17$), comprised of 11 model features; the classifier using the genes GNAS, NOTCH1, SMAD4, and TET1 displayed the highest area under the curve (AUC) of 0.924 with F1 score of 0.880; the ROC curve represents the performance of the classification model at the true positive rate (TPR, or sensitivity) versus the false positive rate (FPR, or 1 − specificity) to classify tumor specimens into the clinical histology grade; the F1 score is the harmonic mean of precision and recall (sensitivity or TPR)

Funding Johns Hopkins AHN Cancer Research Alliance Grant, National Human Genome Research Institute of the National Institutes of Health, R01HG010589, Claude-Worthington Benedum Foundation Award, Pittsburgh Foundation, Highmark Health

Disclosure This work was performed as part of the AHNCI Moonshot Biomarker Program and supported in part by Highmark Health. Partial support was provided by: Johns Hopkins-AHN Cancer Research Alliance Grant (WAL), Pittsburgh Foundation (PLW), The Appendix Cancer Pseudomyxoma Peritonei Research Foundation (PLW), the Claude-Worthington Benedum Foundation Award (WAL), and National Human Genome Research Institute of the National Institutes of Health under award no. R01HG010589 (RS). These funding sources had no role in the study design, data collection, analysis, interpretation of the data, and writing of the manuscript, and do not necessarily represent the official views of the National Institutes of Health.

References

1. Belmont et al. (2024). Circulating tumor DNA effectively predicts recurrence and treatment response in appendiceal cancer. *Ann Surg* (in press).
2. Dhiman, et al. Tumor-informed personalized ctDNA assay informs recurrence in colorectal and high-grade appendiceal peritoneal metastases. *Ann Surg*. 2023;278(6):925–31.
3. Singh et al., 2024. Highly sensitive ctDNA assay aids management of radiographically occult peritoneal metastases. *JCO Precis Oncol* (in press).
4. White et al., 2025. The landscape of circulating tumor DNA in metastatic appendiceal cancer. *JCO Precis Oncol* (in press).
5. Doll J, et al. Molecular profiling of low-grade appendiceal mucinous neoplasms (LAMN). *Genes Chromosomes Cancer*. 2024;63(10):e23270. https://doi.org/10.1002/gcc.23270. (**PMID: 39400480**).
6. Ang CSP, et al. Genomic landscape of appendiceal neoplasms. *JCO Precis Oncol*. 2018. https://doi.org/10.1200/PO.17.00302.
7. Tokunaga R, et al. Molecular profiling of appendiceal adenocarcinoma and comparison with right-sided and left-sided colorectal cancer. *Clin Cancer Res Off J Am Assoc Cancer Rese*. 2019;25(10):3096–103. https://doi.org/10.1158/1078-0432.CCR-18-3388.
8. Foote, et al. The impact of germline alterations in appendiceal adenocarcinoma. *Clin Cancer Res*. 2023;29(14):2631–7.
9. Foote MB, et al. Germline alterations influence histologic grade and survival outcomes in appendiceal adenocarcinoma. *Clin Cancer Res*. 2023;29(14):2631–7.
10. LaFramboise WA, Petrosko P, Gallo PH, Gil L, Lam TL, Barr RM, Schumacher PE, Kharoud HK, Taylor KM, Dalton E, Bapat B, Patel S, Nakayama J, Hilton CJ, Ercolano LB, Zaidi AH, Allen CJ, Rachman T, Carja O, Schwartz R, Wagner PL, Bartlett DL. Cell-Free DNA, Tumor molecular concordance, and clinical correlates of patients with cancer treated in a large community health care network. *J Mol Diagn*. 2025. https://doi.org/10.1016/j.jmoldx.2025.05.007. (**PMID: 40578550**).
11. Pestinger V, et al. Use of an integrated pan-cancer oncology enrichment next-generation sequencing assay to measure tumour mutational burden and detect clinically actionable variants. *Mol Diagn Ther*. 2020;24(3):339–49.
12. Chakravarty D, Gao J, Phillips SM, Kundra R, Zhang H, Wang J, Rudolph JE, Yaeger R, Soumerai T, Nissan MH, Chang MT, Chandarlapaty S, Traina TA, Paik PK, Ho AL, Hantash FM, Grupe A, Baxi SS, Callahan MK, Snyder A, Chi P, Danila D, Gounder M, Harding JJ, Hellmann MD, Iyer G, Janjigian Y, Kaley T, Levine DA, Lowery M, Omuro A, Postow MA, Rathkopf D, Shoushtari AN, Shukla N, Voss M, Paraiso E, Zehir A, Berger MF, Taylor BS, Saltz LB, Riely GJ, Ladanyi M, Hyman DM, Baselga J, Sabbatini P, Solit DB, Schultz N. OncoKB: a precision oncology knowledge base. *JCO Precis Oncol*. 2017. https://doi.org/10.1200/PO.17.00011. (**PMID: 28890946; PMCID: PMC5586540**).
13. Robinson JT, Thorvaldsdóttir H, Wenger AM, Zehir A, Mesirov JP. Variant review with the integrative genomics viewer. *Cancer Res*. 2017;77(21):e31–4. https://doi.org/10.1158/0008-5472.CAN-17-0337. (**PMID:29092934; PMCID:PMC5678989**).
14. Asare EA, Compton CC, Hanna NN, Kosinski LA, Washington MK, Kakar S, Weiser MR, Overman MJ. The impact of stage, grade, and mucinous histology on the efficacy of systemic chemotherapy in adenocarcinomas of the appendix: analysis of the National Cancer Data Base. *Cancer*. 2016;122(2):213–21. https://doi.org/10.1002/cncr.29744. (**PMID: 26506400; PMCID: PMC4860278**).
15. Constantin M, et al. Landscape of genetic mutations in appendiceal cancers. *Cancers*. 2023;15(14):3591. https://doi.org/10.3390/cancers15143591.
16. Hara K, Saito T, Hayashi T, et al. A mutation spectrum that includes GNAS, KRAS and TP53 may be shared by mucinous neoplasms of the appendix. *Pathol Res Pract*. 2015;211(9):657–64. https://doi.org/10.1016/j.prp.2015.06.004.
17. LaFramboise WA, Pai RK, Petrosko P, Belsky MA, Dhir A, Howard PG, Becich MJ, Holtzman MP, Ahrendt SA, Pingpank JF, Zeh HJ, Dhir R, Bartlett DL, Choudry HA. Discrimination

of low- and high-grade appendiceal mucinous neoplasms by targeted sequencing of cancer-related variants. *Mod Pathol*. 2019;32(8):1197–209. https://doi.org/10.1038/s41379-019-0256-2. (**Epub 2019 Apr 8 PMID: 30962504**).

18. Hawsawi YM, Shams A, Theyab A, Abdali WA, Hussien NA, Alatwi HE, Alzahrani OR, Oyouni AAA, Babalghith AO, Alreshidi M. BARD1 mystery: tumor suppressors are cancer susceptibility genes. *BMC Cancer*. 2022;22(1):599. https://doi.org/10.1186/s12885-022-09567-4.PMID:35650591;PMCID:PMC9161512.
19. Miao K, Lei JH, Valecha MV, Zhang A, Xu J, Wang L, Lyu X, Chen S, Miao Z, Zhang X, Su SM, Shao F, Rajendran BK, Bao J, Zeng J, Sun H, Chen P, Tan K, Chen Q, Wong KH, Xu X, Deng CX. NOTCH1 activation compensates BRCA1 deficiency and promotes triple-negative breast cancer formation. *Nat Commun*. 2020;11(1):3256. https://doi.org/10.1038/s41467-020-16936-9. (**PMID:32591500; PMCID:PMC7320176**).
20. Zhu X, Salhab M, Tomaszewicz K, et al. Heterogeneous mutational profile and prognosis conferred by TP53 mutations in appendiceal mucinous neoplasms. *Hum Pathol*. 2019;85:260–9. https://doi.org/10.1016/j.humpath.2018.11.011.
21. Gao J, Aksoy BA, Dogrusoz U, Dresdner G, Gross B, Sumer SO, Sun Y, Jacobsen A, Sinha R, Larsson E, Cerami E, Sander C, Schultz N. Integrative analysis of complex cancer genomics and clinical profiles using the cBioPortal. *Sci Signal*. 2013;6(269):l1. https://doi.org/10.1126/scisignal.2004088. (**PMID: 23550210; PMCID: PMC4160307**).
22. Baumgartner, et al. Prognostic value of circulating tumor DNA in patients undergoing CRS/HIPEC for peritoneal carcinomatosis. *Ann Surg Oncol*. 2020;28(4):198–206.